

Electronic Supplementary Information (ESI)

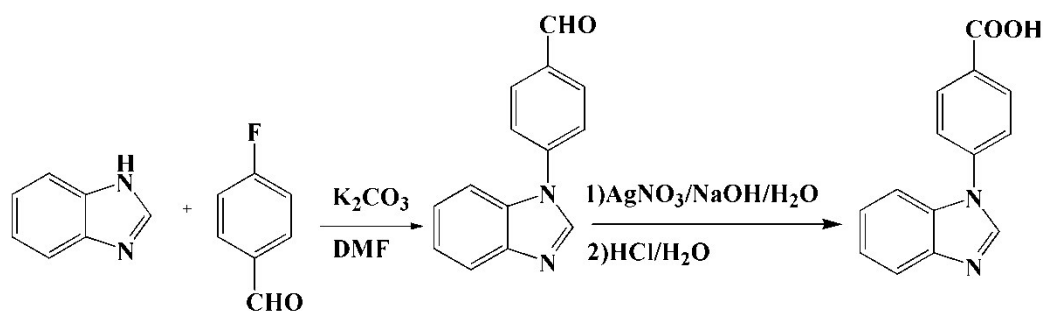
3D Chiral and 2D achiral cobalt(II) compounds constructed of 4-(benzimidazole-1-yl)benzoic Ligand exhibiting field-induced single-ion-magnet-type slow magnetic relaxation

Yu-Ling Wang,^a Lin Chen,^a Cai-Ming Liu,^b Zi-Yi Du,^c Li-Li Chen^a and Qing-Yan Liu^{*,a}

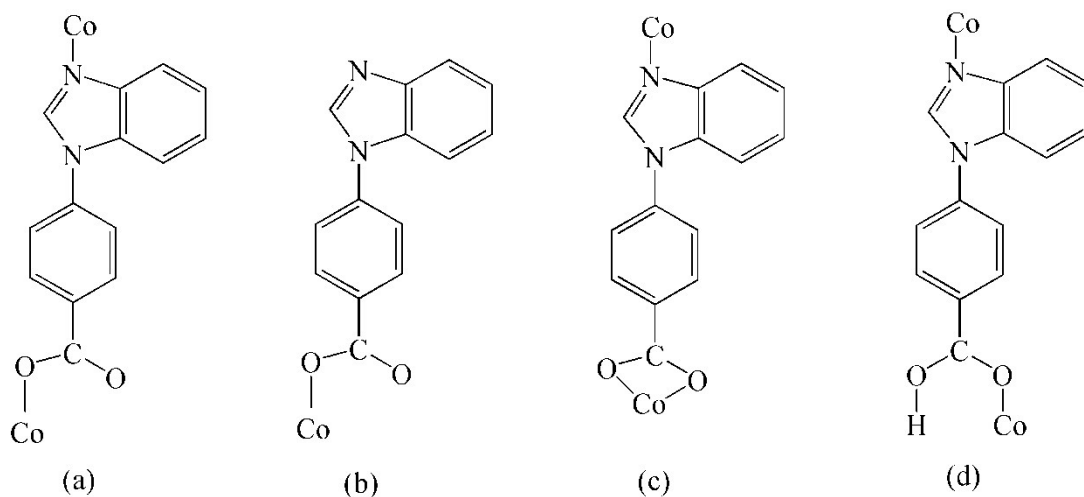
^a College of Chemistry and Chemical Engineering, Jiangxi Normal University, Nanchang 330022, P. R. China

^b Beijing National Laboratory for Molecular Sciences, Institution of Chemistry, Chinese Academy of Sciences, Center for Molecular Sciences, Beijing 100190, P. R. China

^c College of Chemistry and Chemical Engineering, Gannan Normal University, Ganzhou 341000, P. R. China.



Scheme S1. Preparation of Hbmzbc ligand.



Scheme S2. Coordination modes of Hbmzbc ligand in **1** and **2**.

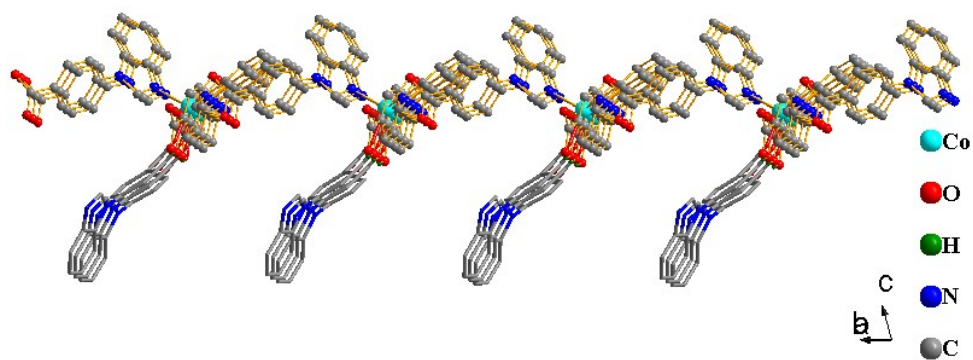
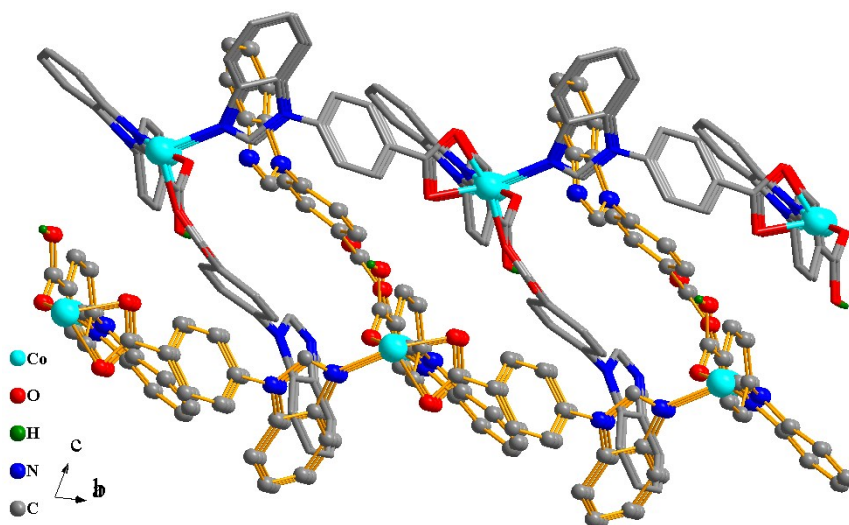


Figure S1 The 2D layered structure of **2** view along *a* axis showing the terminal bmzbc^- ligands (wires mode) as suspensions hang at one side of the layer.



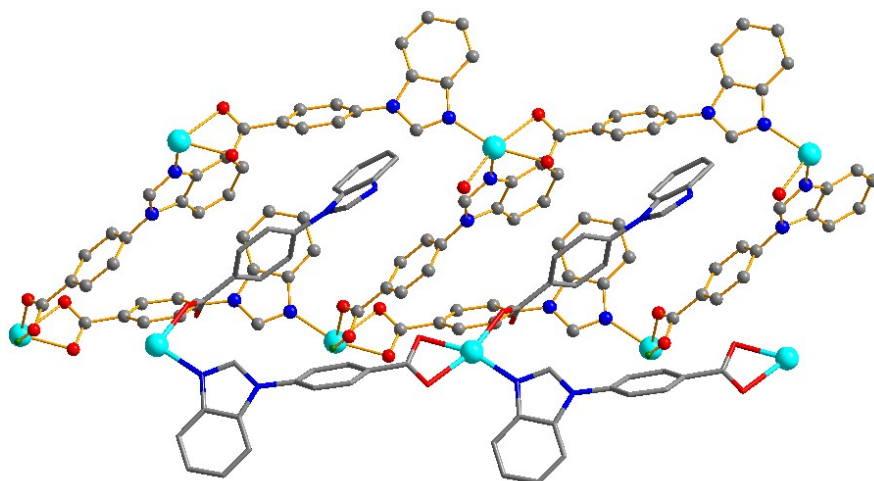


Figure S2 Two neighboring layers discriminated by ball and wire modes, respectively, are interdigitated with each other through the hanging bmzbc^- ligands penetrating into the naosized cavities of the metal-organic squares in **2**.

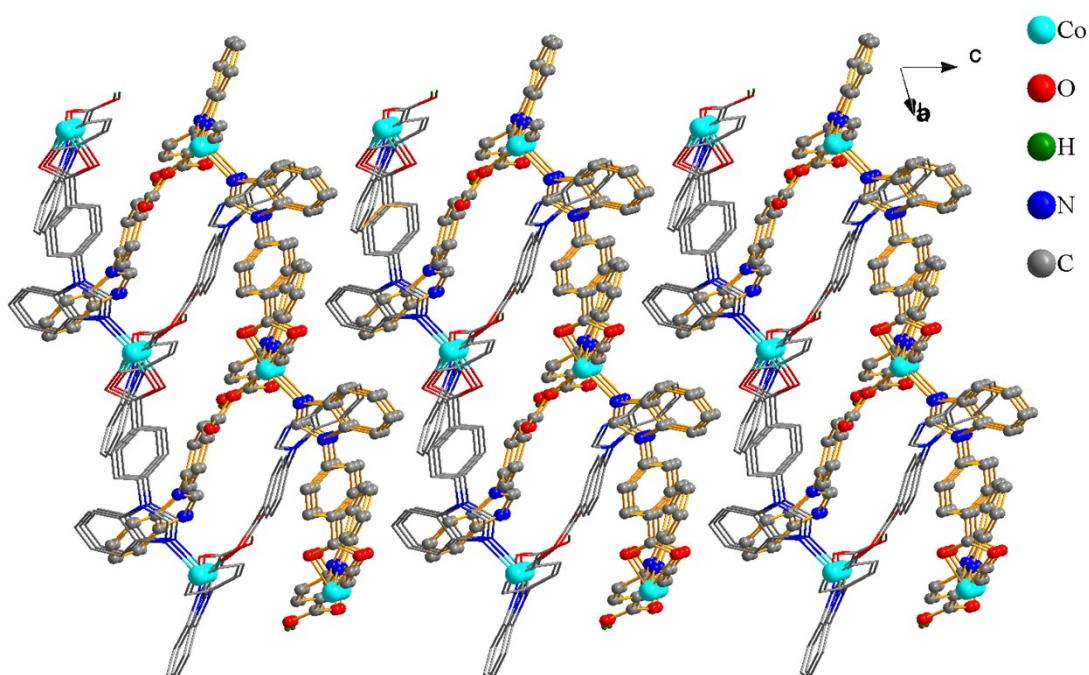


Figure S3 The two interdigitated layers discriminated by ball and wire modes, respectively, are packed along the c direction to generate a 3D packing.

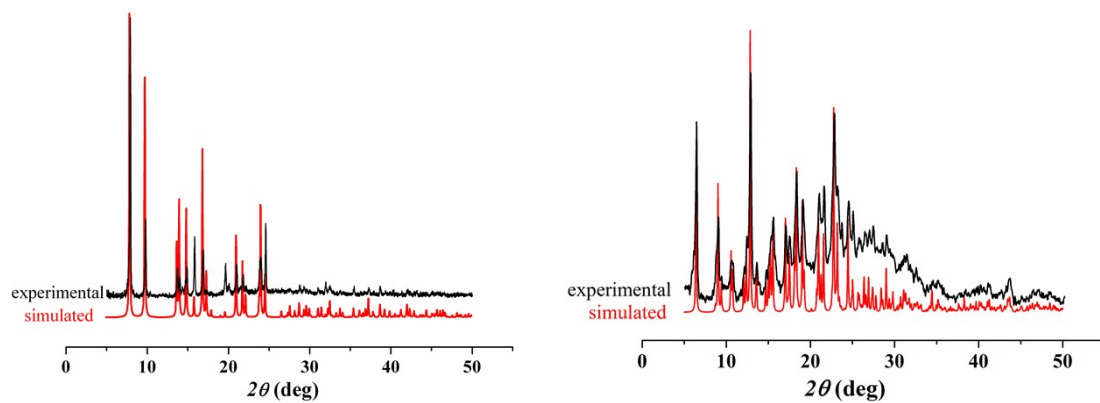


Figure S4 Simulated and experimental powder X-ray diffraction patterns for **1** (left) and **2** (right).

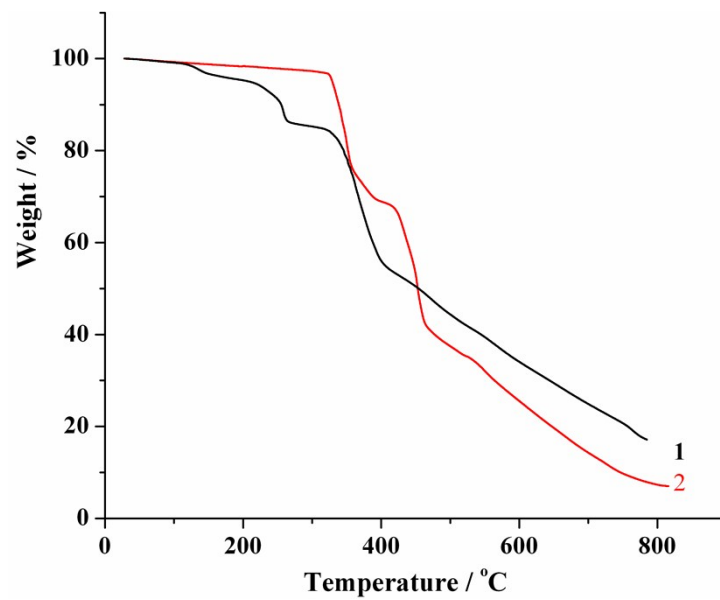


Figure S5 TGA curve for **1** and **2**.

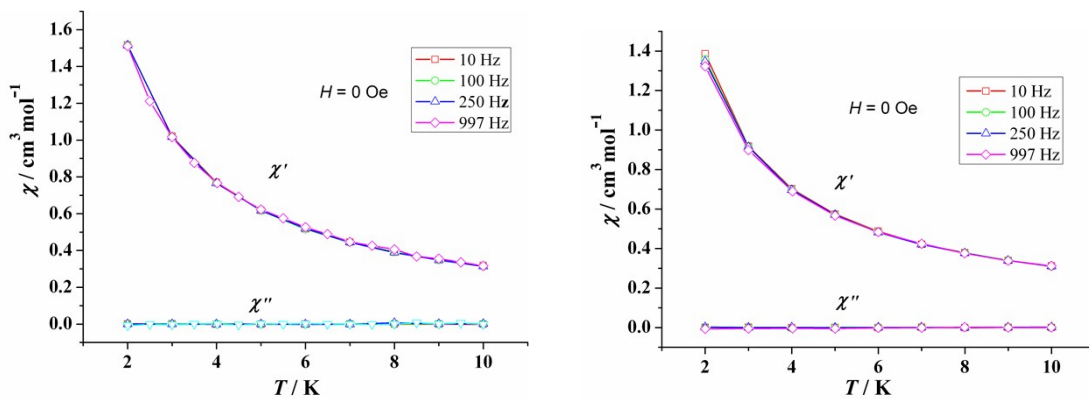


Figure S6 Temperature dependence of in-phase (χ') and out-of-phase (χ'') of **1** (left) and **2** (right) at different frequencies in the absence of dc field, no obvious frequency dependence can be observed.

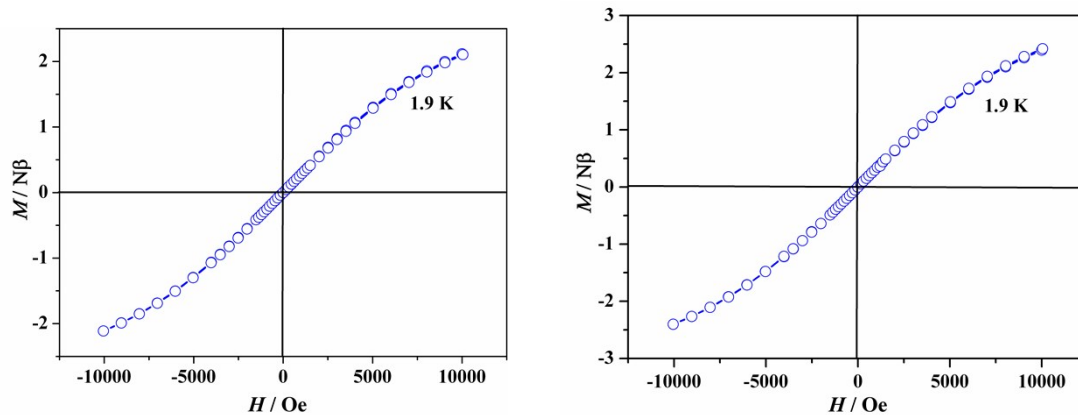


Figure S7 Field dependence of the magnetization of **1** (left) and **2** (right) measured at 1.9 K.

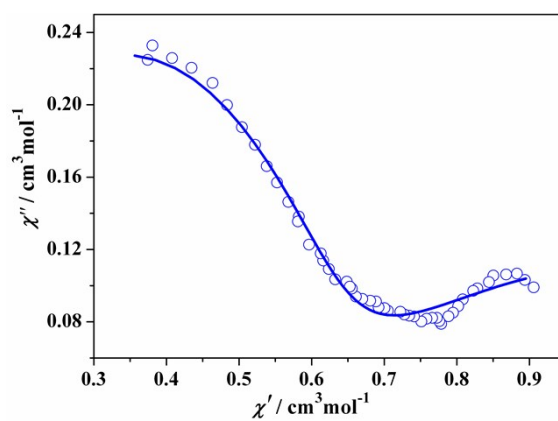


Figure S8. Cole-Cole plots for **1** under 2 kOe dc field. The solid lines are the best fit obtained with a sum of two modified Debye functions Debye model.

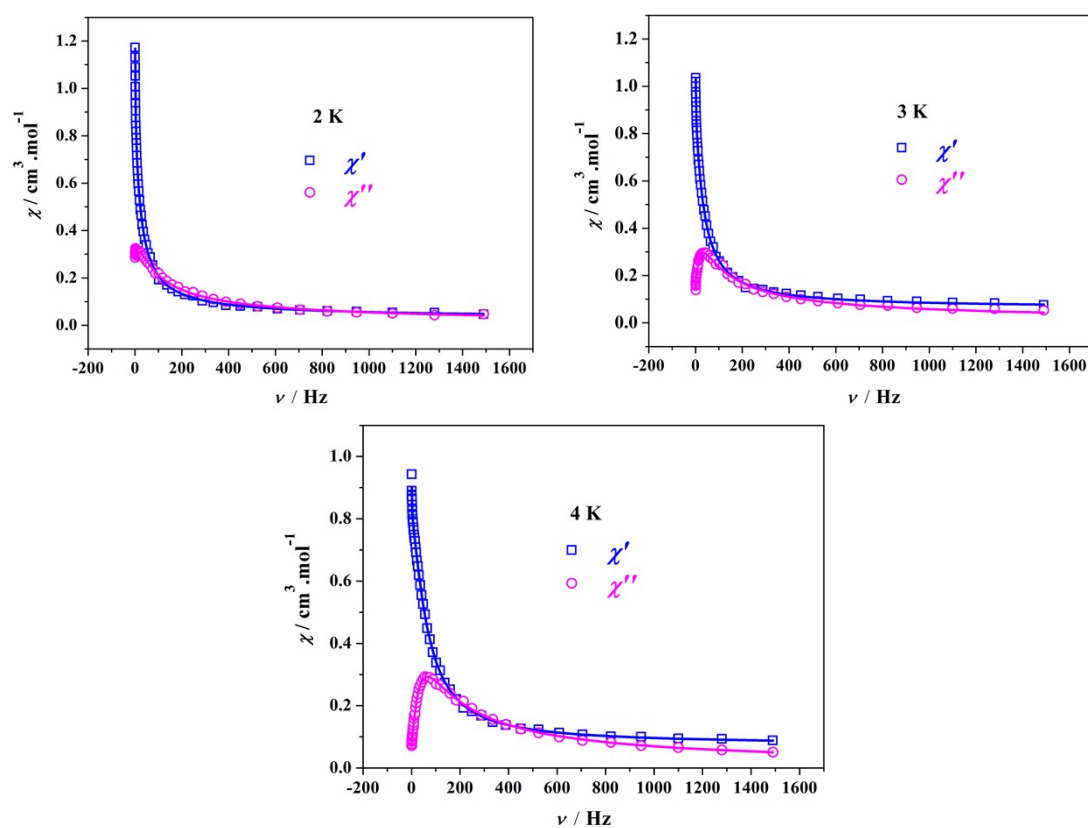


Figure S9. Frequency dependence of the in-phase (χ' , top) and out-of-phase (χ'' , bottom) ac susceptibility of **2** at different temperatures. The solid lines represent the best fitting with the sum of two modified Debye functions.

Equations:

(a) The sum of two modified Debye functions:

$$\chi_{\text{ac}}(\omega) = \frac{\chi_2 - \chi_1}{1 + (i\omega\tau_2)^{(1-\alpha_2)}} + \frac{\chi_1 - \chi_0}{1 + (i\omega\tau_1)^{(1-\alpha_1)}} + \chi_0 \quad (\text{equ S1})$$

Both the χ' versus T plot and the χ'' versus T plot were fitted to equation S1 synchronously, affording seven parameters χ_1 , χ_2 , χ_0 , α_1 , α_2 , τ_1 and τ_2 at each temperature. The results are listed in Table S1 and depicted as Fig. S9.

Table S1. Linear combination of two modified Debye model fitting parameters from 2 K to 4 K of **2** under 2k Oe dc field.

$T(\text{K})$	$\chi_2(\text{cm}^3.\text{mol}^{-1})$	$\chi_1(\text{cm}^3.\text{mol}^{-1})$	$\chi_0(\text{cm}^3.\text{mol}^{-1})$	$\tau_1(\text{s})$	α_1	$\tau_2(\text{s})$	α_2	R
2	1.36995	0.47777	0.02578	0.1177	0.00003	0.00628	0.28304	1.6×10^{-4}
3	1.11036	0.28482	0.05833	0.09118	0.00997	0.00428	0.23058	3.1×10^{-4}
4	0.93571	0.19492	0.0714	0.08305	0.02639	0.00238	0.15692	3.7×10^{-4}